WWW.IJRPR.COM

International Journal of Research Publication and Reviews

Journal homepage: www.ijrpr.com ISSN 2582-7421

Design and Structural Analysis of Rocket Convergent – Divergent Nozzle

Nitin Kumar Gummadidala[1], Gunda Shiva Krishna[2], B D Y Sunil[3]

[1]Dept. of Aerospace Engineering. Institute of Aeronautical Engineering, Hyderabad, India nitinshalivahana01998@gmail.com
[2]Dept. of Aerospace Engineering, Institute of Aeronautical Engineering, Hyderabad, India g.shivakrishna@iare.ac.in
[3]Dept. of Aerospace Engineering, Institute of Aeronautical Engineering, Hyderabad, India bdy.sunil@iare.ac.in

ABSTRACT—

A rocket engine nozzle is a critical component used to expand and accelerate combustion gases to high supersonic speeds. The optimal nozzle size is achieved when the exit pressure matches the ambient pressure. The throat of the nozzle experiences significantly higher pressure than the ambient environment, along with substantial internal stress due to the extreme thrust forces and high temperatures generated during engine ignition. This study focuses on designing and conducting a structural analysis of a convergent-divergent nozzle made from two different materials: Titanium Carbide and Titanium Alloy Ti6Al4V. The nozzle geometry and applied loads remain consistent for both materials. The material performance is evaluated based on total deformation and Von Mises stress. The design of the convergent-divergent nozzle is created using CATIA V5, with its geometry sourced from literature. Structural analysis is carried out in ANSYS Workbench to assess the effects of pressure loads, gas flow, ambient pressure, and temperature on the nozzle.

Keywords— CATIA V5, ANSYS, Convergent-Divergent Nozzle, Throat, Titanium Carbide, Titanium Alloy Ti-6Al-4V.

1. Introduction

The combustion of solid rocket propellant generates hot, high-energy gases that serve as a reservoir of potential energy, which must be efficiently converted into kinetic energy to propel the rocket from launch to its intended destination. Without effective utilization, much of this energy would be lost as heat dissipating into the surrounding atmosphere. The rocket nozzle plays a crucial role in this process by converting exhaust gas energy into kinetic energy, which is then transformed into thrust.

Functioning as a metering device for the propulsion system, the nozzle regulates gas flow rates and ensures a consistent thrust output over a specified time frame. This energy conversion occurs as the gas molecules are accelerated to extremely high velocities upon exiting the motor.

The total mass of the hot gases produced during combustion is equivalent to the initial mass of the solid propellant being burned. Once ignited, these gases rapidly fill the combustion chamber, increasing the pressure to an operational level where a steady amount of exhaust products is generated. Although it may not be immediately obvious, the nozzle facilitates gas acceleration by restricting free flow, utilizing a smaller exit cross-sectional area compared to the chamber to optimize thrust production.

A. Convergent-Divergent Nozzle

The convergent-divergent nozzle, available in two primary configurations—external and submerged—is widely used in solid-propellant rocket engines. Another variation, known as the "spike" nozzle, has been under development for some time but is primarily utilized in experimental motors. This design allows for thrust magnitude and chamber pressure control, enabling stop capability and precise thrust modulation for missile applications that require variable thrust levels at different flight stages.

The external configuration is the simplest form of the convergent-divergent nozzle, with the entire motor positioned externally. In contrast, the submerged configuration integrates the nozzle inlet, throat, and a portion of the nozzle structure within the motor chamber in a cantilevered arrangement.

Types of Nozzle: The submerged configuration is the more complex of the two, as both its medial and lateral surfaces are directly exposed to hot gases. In addition to the forces generated by gas flow along its internal surfaces, the submerged section must also withstand external pressure forces.Additionally, the most common nozzle exit designs are conical and contoured. The purpose of contouring is to regulate the exhaust stream, ensuring that the thrust is directed as closely as possible along the nozzle's longitudinal centerline. This design minimizes flare and divergence, effectively concentrating the thrust for optimal performance.

External Submerged Spike

Fig. 1.1: External, Submerged, Spike nozzle.

Exhaust gas velocity: As gas enters the nozzle, it initially moves at subsonic speeds. Due to the decreasing cross-sectional area, the gas accelerates until it reaches sonic velocity at the throat, the narrowest section of the nozzle. Beyond the throat, as the area expands, the gas continues to accelerate, reaching supersonic velocities.

The velocity of the exhaust gases at the nozzle exit can be determined using the following equation:

$$v_{exit} = \sqrt{\frac{2\gamma}{\gamma - 1} R T_0} \left(1 - \left(\frac{P_{exit}}{P_0} \right)^{\frac{\gamma - 1}{\gamma}} \right)$$

Where:

- v_{exit} = Exit velocity of exhaust gases
- γ = Ratio of specific heats (C_p/C_v)
- R = Specific gas constant
- T_0 = Stagnation temperature
- P_{exit} = Exit pressure
- P_0 = Stagnation pressure

B. Flow Pattern

As the flow exits the combustion chamber, it accelerates through the converging section, reaching its highest subsonic velocity at the nozzle throat. It then decelerates through the diverging section and exits into the ambient environment as a subsonic jet. Reducing the back pressure increases the flow speed throughout the nozzle. If the back pressure is reduced sufficiently, the flow at the throat reaches Mach 1, creating a condition known as choked flow. In this state, further reductions in back pressure do not shift the location of Mach 1 away from the throat, but they do alter the flow behavior in the diverging section.

When the back pressure drops just below the critical level for choking, a supersonic flow region forms immediately downstream of the throat. Unlike subsonic flow, supersonic flow accelerates as the cross-sectional area increases. This acceleration is eventually interrupted by a normal shock wave, which causes an abrupt deceleration back to subsonic speeds. The subsonic flow then continues decelerating through the remainder of the nozzle and exits as a subsonic jet. In this regime, adjusting the back pressure alters the length of the supersonic region before the shock wave.

If the back pressure is reduced further, the supersonic region extends along the nozzle until the shock wave reaches the nozzle exit. In this scenario, the flow reaches very high speeds before encountering the shock, but after passing through it, the jet remains subsonic. Lowering the back pressure even more causes the shock to extend into the exhaust jet, creating a complex system of shocks and reflections that result in a mixture of subsonic and supersonic regions.

If the back pressure is sufficiently low, the jet may become entirely supersonic. Because the shock is no longer perpendicular to the nozzle walls, it deflects the flow inward as it exits, leading to an initially contracting jet. This condition, known as overexpanded flow, occurs when the exit pressure is lower than the ambient pressure, meaning the nozzle has expanded the flow more than necessary.

Further reductions in back pressure weaken the shock wave pattern in the jet. When the back pressure equals the exit pressure, the shocks disappear entirely, and the jet remains uniformly supersonic—this is known as the "design condition," as it is often the desired operating state.

If the back pressure is reduced beyond this point, a new imbalance arises where the exit pressure exceeds the ambient pressure. This condition, known as under expanded flow, leads to the formation of expansion waves at the nozzle exit. These waves cause the jet edges to turn outward, forming a plume and introducing a different complex wave pattern in the exhaust flow.

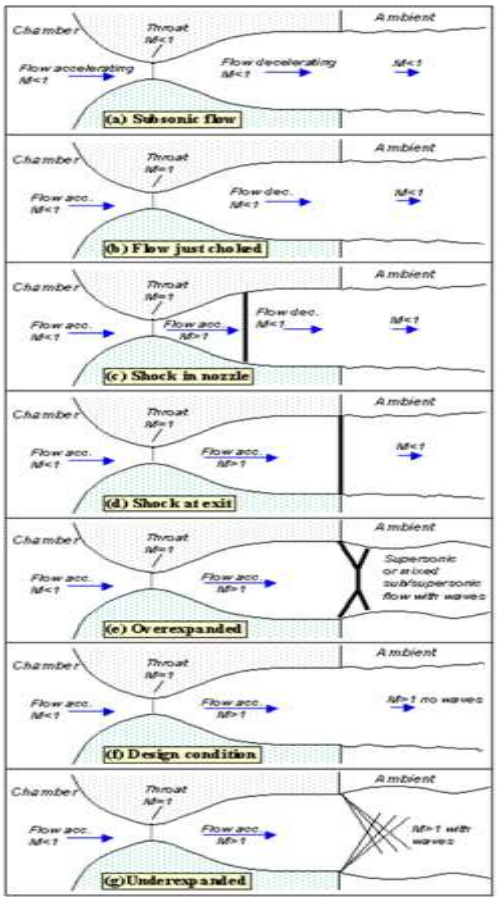

Fig. 1.2: Flow Patterns.

2. Literature survey

A. Introduction

The aerospace industry has witnessed remarkable advancements over the past decades, driven by technological innovations, material science improvements, and computational developments. Aerospace engineering encompasses a broad spectrum of disciplines, including aerodynamics, propulsion systems, structural mechanics, avionics, and space exploration. The continuous quest for efficiency, safety, and sustainability has led to extensive research in areas such as lightweight composite materials, advanced flight control systems, and next-generation propulsion technologies.

B. Design and Analysis of rocket nozzle to determine optimum material and fuel

Santhosh Reddy [1] This study focuses on the design, modeling, and structural analysis of rocket nozzles to determine the optimal nozzle configuration and material selection. The nozzles were designed using Rocket Propulsion Analysis software, modeled in SolidWorks, and analyzed in ANSYS to evaluate their structural integrity and performance. Key geometric parameters, including area expansion ratio, throat diameter, and nozzle type, significantly influence nozzle efficiency. The impact of the area expansion ratio on performance is examined in detail. Since different nozzle

designs exhibit varying characteristics; the type of nozzle indirectly affects the thrust generation. As exhaust gases pass through the nozzle, the pressure energy of the combustion products is converted into kinetic energy, generating the thrust necessary for liftoff.

C. Analysis of Rocket Nozzle using Methods of Characteristics

Vinayak H. Khatawate [2] This study presents the design of a minimum-length nozzle using the Method of Characteristics (MOC) approach. The calculations assume compressible, isentropic gas flow. To ensure the structural integrity and safety of the nozzle, a thermo-structural analysis is conducted. Three different materials are evaluated and compared based on the stresses and deformations determined through Finite Element Analysis (FEA). Additionally, two commonly used cooling techniques—regenerative and film cooling—are considered. A Computational Fluid Dynamics (CFD) analysis is performed to assess the effectiveness of film cooling in reducing temperature.

D. Design and Analysis *of a Rocket C-D Nozzle*

Jayaprakash P[3] The nozzle design is developed using previous designs as benchmarks. With the growing demand for rocket propulsion in applications such as manned space missions and satellite launches, optimizing nozzle performance is essential. To achieve this, a fundamental design is

created based on compressible flow principles. Key parameters such as temperature, pressure, and velocity are analyzed at different sections of the nozzle to determine its shape, insulation, and cooling requirements, as well as to calculate the thrust.

Both theoretical calculations and Computational Fluid Dynamics (CFD) simulations are performed to validate the design. The results from these methods—simulation and theoretical analysis—are compared to evaluate their accuracy. Additionally, the findings obtained from ANSYS Fluent simulations are analyzed alongside theoretical calculations to ensure precision and reliability.

E. Design and Analysis of Rocket Nozzle

R. Harikrishna[4] This study focuses on the design and analysis of two different rocket nozzle configurations. The first configuration features a basic design without fillets or curved surfaces, while the second incorporates fillets and curved surfaces to reduce stress concentrations. The second configuration is chosen because, without an optimized geometry, high-stress concentrations can develop at sharp corners, potentially compromising structural integrity.

The fillet radii are determined based on previous research conducted by academicians and design experts to achieve an optimized configuration that minimizes overall induced stress and enhances nozzle lifespan. Both the initial and optimized configurations are modeled in ANSYS Mechanical APDL 14.5, using the coupled element Quad 8-node 223 for analysis. The selected material for the study is Ti6Al4V (Grade 5).

F. Time-Frequency Analysis of Rocket Nozzle Wall Pressures during Start-up Transients.

Woutijn J. Baars[5] Fluctuating wall pressure surveys were performed on a sub-scale, thrust-optimized parabolic nozzle to investigate its Fourier-azimuthal mode behavior under both fixed and transient start-up conditions. These unsteady flow characteristics are influenced by shock wave interactions with the turbulent boundary layer, which are dependent on the nozzle pressure ratio and geometry. The results indicate that at low nozzle pressure ratios, where the flow exists in a Free Shock Separation state, strong spectral similarities are observed between fixed and transient conditions.

3. METHODOLOGY

Introduction

Structural analysis is a fundamental aspect of engineering that focuses on evaluating the strength, stability, and durability of structures under various loading conditions. It involves assessing how materials and components respond to forces such as tension, compression, shear, and thermal stresses to ensure safe and efficient designs.

In engineering applications, structural analysis is crucial for predicting how a structure will perform before it is built. It helps in identifying potential weaknesses, optimizing material selection, and improving overall structural efficiency. Various methods, including analytical calculations, Finite Element Analysis (FEA), and computational simulations, are used to analyze different structural components.

Materials

In this study, two different materials are analyzed using the same nozzle geometry and applied loads to compare their performance. The objective is to evaluate the structural behavior of each material under identical conditions and determine variations in factors such as stress distribution, deformation, and overall efficiency.

1. Titanium carbide (TiC) is a hard, refractory ceramic material known for its exceptional mechanical properties, including high hardness, wear resistance, and thermal stability. It is widely used in aerospace, automotive, and industrial applications due to its ability to withstand extreme conditions. TiC exhibits excellent corrosion resistance, making it suitable for high-temperature environments and abrasive wear applications.

TABLE 1: Properties of the Titanium Carbide

Parameters	**Values**	**Units**
Density	4.93	g/cm^3
Melting Point	3140	℃
Boiling Point	4820	℃
Young's Modulus	400	GPa
Shear Modulus	188	GPa
Hardness Hv	30	GPa
Molar Mass	59.878	$g.mol^{-1}$
Magnetic Susceptibility	+8.0 x 10^{-6}	cm^3/mol

2. Titanium alloy Ti-6Al-4V is one of the most widely used titanium alloys due to its excellent combination of strength, corrosion resistance, and lightweight properties. Composed primarily of titanium, it contains 6% aluminum and 4% vanadium, which enhance its mechanical characteristics and heat resistance. This alloy is commonly used in aerospace, medical implants, and automotive applications, where high performance under extreme conditions is essential. Ti-6Al-4V is known for its high strength-to-weight ratio, good fatigue resistance, and biocompatibility, making it a preferred material in industries requiring durability and reliability.

TABLE 2: Properties of Titanium alloy Ti-6Al-4V

Parameters	**Values**	**Units**
Density	4.51	g/cm^3
Melting Point	1660	℃
Boiling Point	2850	℃
Young's Modulus	115	GPa
Fatigue Strength	510	MPa
Tensile Strength	950	GPa
Elongation	15	%
Thermal Conductivity	6.7	W/m-k

Design and Analysis

A convergent-divergent nozzle will be designed using CATIA V5, with its geometry refined based on insights from various literature sources. Surface modeling has been chosen for this design as it offers greater accuracy and consistency compared to wireframe modeling. Additionally, surface models provide extensive geometric details, making them highly suitable for engineering and design applications. The advancement of surface modeling has been driven by the limitations and inefficiencies associated with wireframe modeling.

Meshing of the designed nozzle is carried out using ANSYS 2024 R2, followed by structural analysis in the same software. The analysis is conducted by applying identical pressure and force conditions to nozzles made from two different materials, allowing for a comparative evaluation of their structural performance.

TABLE 3: C-D Nozzle design parameters

S. No.	**Measuring Factors**	**Dimensions**
1	Convergent Radius	100 mm
2	Convergent Curve Radius	30 mm
3	Throat Length	80 mm
4	Divergent Length	194.46 mm
5	Divergent Angle	16°
6	Divergent Slant Length	202.32

Meshing

Structural Meshing is done with Number of divisions on the nozzle at convergent section 150 divisions, Throat section 200 divisions & divergent section 100 divisions.

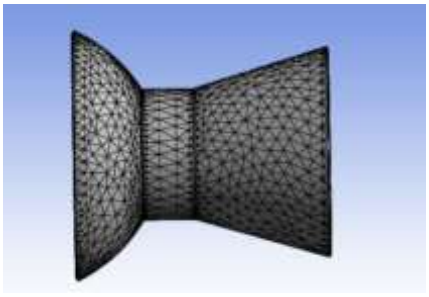

Fig. 3.1: C-D Nozzle Meshing.

4. RESULTS AND DISCUSSIONS

Titanium Carbide

1. Total Deformation

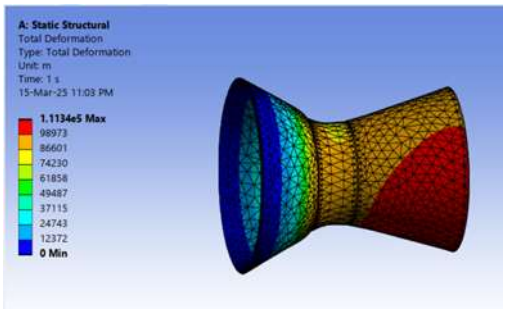

Fig. 4.1: Total deformation of C-D Nozzle.

2. Equivalent Von-mises Stress

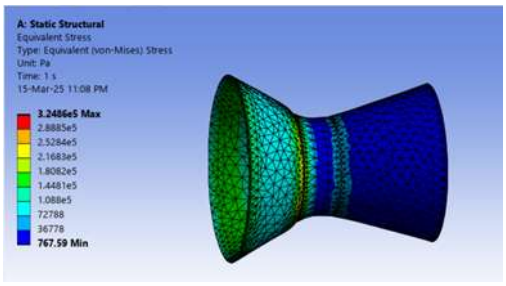

Fig. 4.2: Equivalent Von-mises stress of C-D Nozzle.

3. Maximum Principal Stress

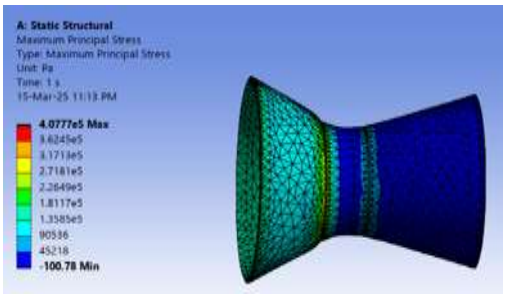

Fig. 4.3: Maximum Principal Stress of C-D Nozzle.

4. Equivalent Elastic Strain

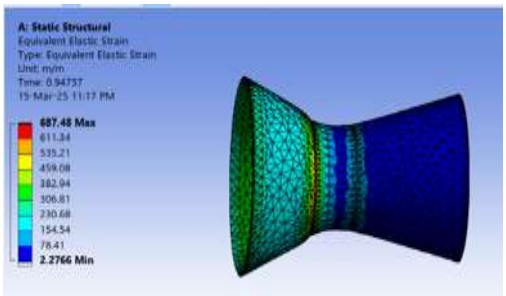

Fig. 4.4: Equivalent Elastic Strain of C-D Nozzle.

5. Maximum Principal Strain

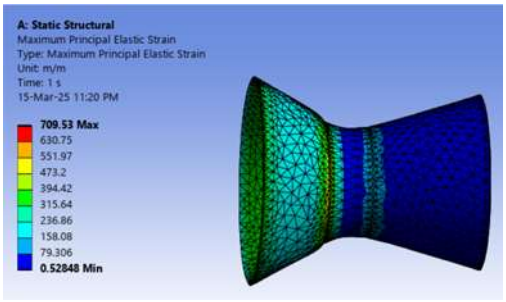

Fig. 4.5: Maximum Principal Strain of C-D Nozzle.

Titanium Alloy Ti-6Al-4V

1. Total Deformation

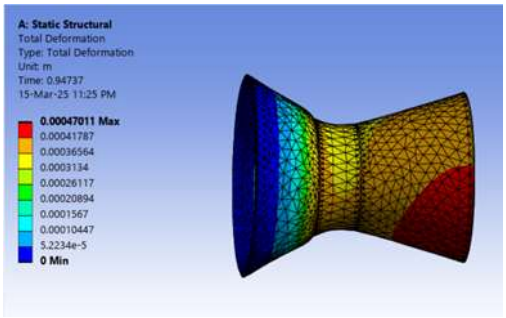

Fig. 4.6: Total Deformation of C-D Nozzle

2. Equivalent Von-mises Stress

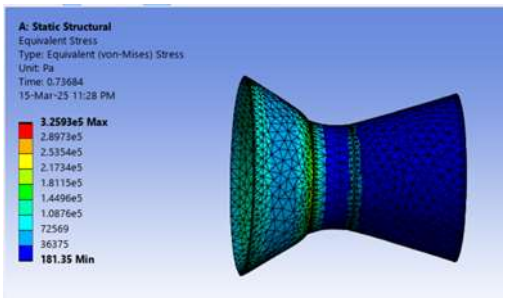

Fig. 4.7: Equivalent Von-mises stress of C-D Nozzle.

3. Maximum Principal Stress

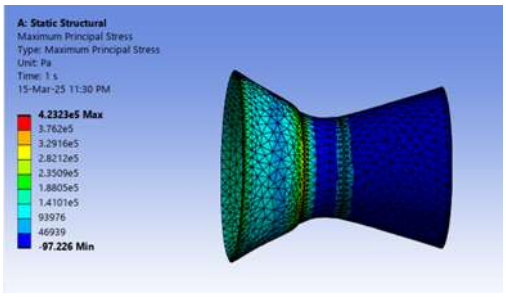

Fig. 4.8: Maximum Principal Stress of C-D Nozzle.

4. Equivalent Elastic Strain

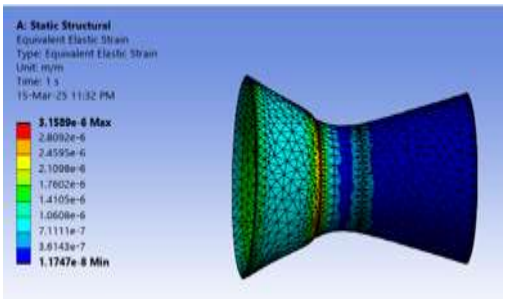

Fig. 4.9: Equivalent Elastic Strain of C-D Nozzle.

5. Maximum Principal Strain

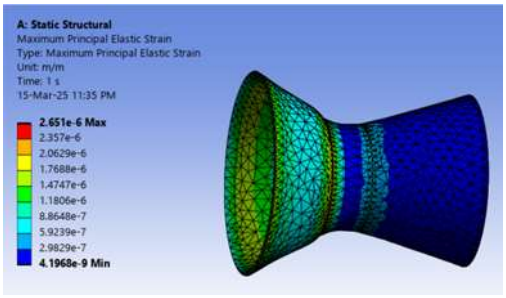

Fig. 4.10: Maximum Principal Strain of C-D Nozzle.

TABLE 4: Nozzle Analysis Values of Both Materials

	Titanium Carbide		**Titanium Alloy Ti-6Al-4V**	
	Min	Max	Min	Max
Total Deformation (mm)	0	165.18	0	256.67
Equivalent Von-mises Stress (MPa)	165.06	482.04	181.35	483.67
Maximum Principal Stress (MPa)	100.7	605.08	97.22	628.08
Equivalent Elastic Strain (mm)	2.276	687.48	$1.1747e^{-8}$	782.78
Maximum Principal Strain (mm)	0.528	709.53	$4.1968e^{-9}$	657.11

The analysis indicates that the deformation of the Titanium Carbide nozzle is lower than that of the Titanium Alloy Ti-6Al-4V nozzle. Both materials exhibit nearly identical von Mises stress values, but the Titanium Carbide experiences lower maximum principal stresses. While the Equivalent Elastic Strain is higher in the Titanium Alloy Ti-6Al-4V, the Maximum Principal Strain is greater in the Titanium Carbide. This comparison highlights how deformation parameters can be utilized to evaluate the performance of different materials when applied to a convergent-divergent nozzle under identical geometric and loading conditions.

Here, we present a comprehensive analysis of the graphical representations for both materials, illustrating their behavior across various parameters in detail.

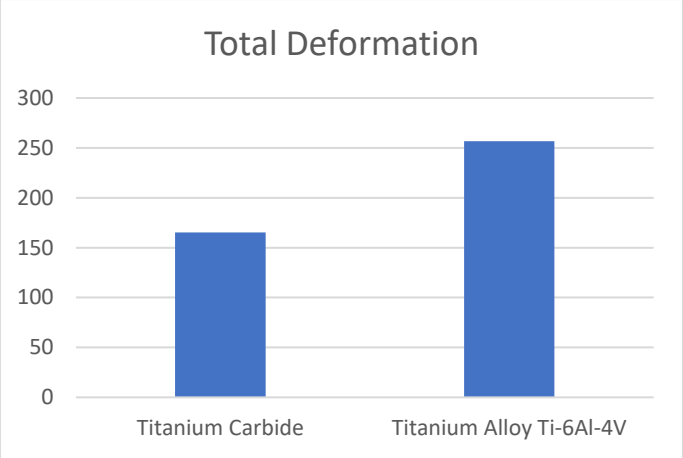

Fig. 4.11: Total deformation graph of Both Nozzle.

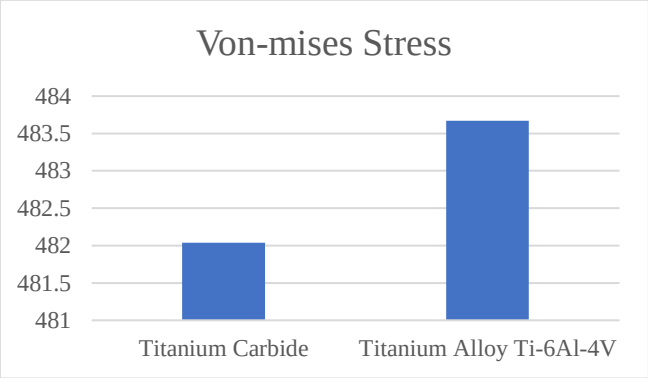

Fig. 4.12: Von-mises Stress graph of Both Nozzle.

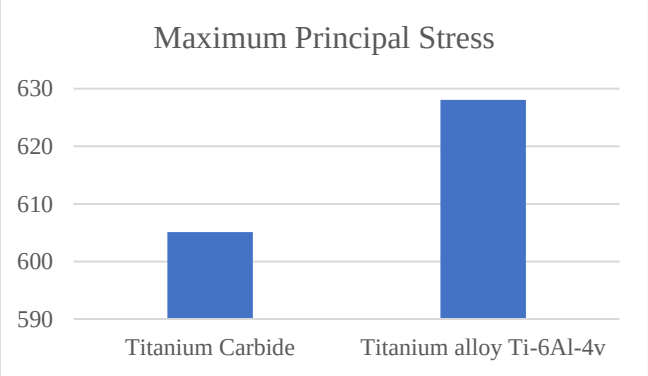

Fig. 4.13: Maximum Principal Stress graph of Both Nozzle.

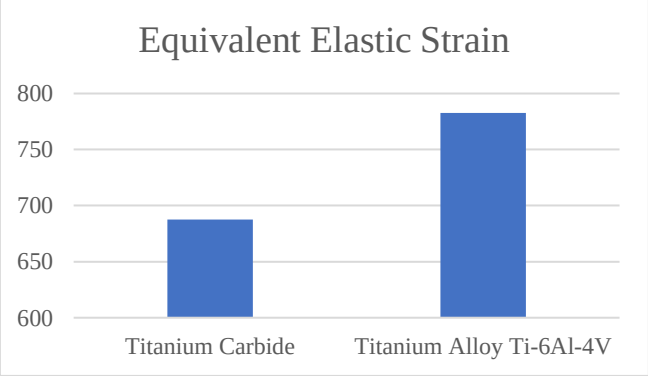

Fig. 4.14: Equivalent Elastic Strain graph of Both Nozzle.

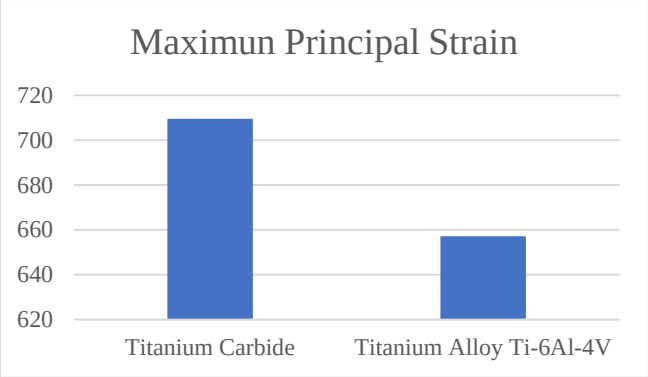

Fig. 4.15: Maximum Principal Strain graph of Both Nozzle.

5. Conclusion

This study provides a comprehensive structural analysis of a convergent-divergent rocket nozzle using Titanium Carbide and Titanium Alloy Ti6Al4V. By maintaining consistent geometry and loading conditions, the performance of both materials was evaluated based on total deformation and Von Mises stress. The results, obtained through ANSYS Workbench simulations, offer valuable insights into how these materials respond to extreme pressure, temperature, and thrust forces. This analysis aids in selecting the most suitable material for high-performance rocket nozzles, ensuring enhanced durability and efficiency in aerospace applications.

References

[1] Quintao, Karla K. (2012). *Design and Optimization of Nozzle Shapes for Maximum Uniformity of Exit Flow*. FIU Electronic Theses and Dissertations, Paper 779.

[2] Mbuyamba, Jean-Baptiste Mulumba (2013). *Calculation and Design of Supersonic Nozzles for Cold Gas Dynamic Spraying Using MATLAB and ANSYS FLUENT*.

[3] Hagemann, Gerald, Immich, Hans, Nguyen, Thong, & Dunmov, Gennady (1998). *Advanced Rocket Nozzles.* Journal of Propulsion and Power, 14(5).

[4] Bhabha Atomic Research Centre. *Water Channel for Supersonic Flow Investigation.* Chemical Engineering and Technology Group.

[5] Ernawati, E., Baso, Y. S., Hidayanty, H., Syarif, S., Aminuddin, A., & Bahar, B. (2022). *Impact of Anemia Education Using Web-Based SHE Smart on Knowledge, Attitudes, and Practices Among Adolescent Girls.* International Journal of Health & Medical Sciences, 5(1), 44-49. https://doi.org/10.21744/ijhms.v5n1.1831

[6] Aeronautical Engineering Department, Hindustan University. *Design and Optimization of De Laval Nozzle to Prevent Shock-Induced Flow Separation.*

[7] Sutton, George P., & Biblarz, Oscar (2001). *Rocket Propulsion Elements.* Wiley-Interscience, Seventh Edition, pp. 1-99.

[8] Ramamurthy, K. (2012). *Rocket Propulsion.* Macmillan Publishers India, pp. 54-89.

[9] Pandey, K. M., & Yadav, S. K. (2010). *CFD Analysis of a Rocket Nozzle with Two Inlets at Mach 2.1.* Journal of Environmental Research and Development, 5(2), 308-321.

[10] Suryasa, I. W., Rodríguez-Gámez, M., & Koldoris, T. (2022). *Post-Pandemic Health and Its Sustainability: Educational Situation.* International Journal of Health Sciences, 6(1), i-v. https://doi.org/10.53730/ijhs.v6n1.5949\

[11] Çengel, Yunus A., & Cimbala, John M. *Fluid Mechanics.* Tata McGraw-Hill, Second Edition, pp. 853-910.

[12] Sutton, G. P., & Biblarz, O. (2001). *Rocket Propulsion Elements.* Wiley-Interscience, 7th edition, pp. 21-23, 24-33.

[13] Barrere, M., Jaumotte, A., Fraeijs De Veubeke, B., & Vandenkerckhove, J. (1960). *Rocket Propulsion*. Elsevier Publishing Company, Amsterdam, pp. 9-21.

[14] Rao, G. V. R. (1958). *Exhaust Nozzle Contour for Optimization Thrust.* Jet Propulsion, June, pp. 34-38, 40-42.

[15] Bartz, D. R. *Turbulent Boundary Layer Heat Transfer from Rapidly Accelerating Flow of Rocket Combustion Gases and Heated Air.* Jet Propulsion Laboratory, pp. 43-44.

[16] Kurbatskii, K. A., & Lestari, A. *Pressure-Based Coupled Numerical Approach to the Problem of Compressible Flow Through Convergent Conical Nozzles.* ANSYS Inc., Lebanon, NH, USA, p. 8.

[17] Rao, G. V. R., Beck, J. E., & Booth, T. E. *Nozzle Optimization for Space-Based Vehicles.* Boeing/Rocketdyne Propulsion & Power, Canoga Park, CA, AIAA 99-2584, p. 11.

[18] Mern, J., & Agarwal, R. *Numerical Simulation Study of Supersonic Conical Nozzle Exhaust.* Department of Mechanical Engineering and Materials Science, Washington University in St. Louis, pp. 8.

[19] Rao, G. V. R., & Dang, A. L. *Thrust Optimization of Nozzle Contour Including Finite Rate Chemical Kinetics.* Rocketdyne Division, Rockwell International Corporation, Canoga Park, CA, & Physical Research Inc., Irvine, CA, AIAA 92-3729, p. 11.

[20] Simpson, T. W., et al. (1998). *Comparison of Response Surface and Kriging Models for Multidisciplinary Design Optimization.* American Institute of Aeronautics and Astronautics, Vol. 98, pp. 1-16.

[21] Korte, J. J., et al. *Multidisciplinary Approach to Linear Aerospike Nozzle Design.* Journal of Propulsion and Power, Vol. 17, pp. 93-98.

[22] Foque, D., et al. *Effects of Nozzle Type and Spray Angle on Spray Deposition in Ivy Pot Plants.* Pest Management Science, Vol. 67, pp. 199-208.